BALANCE RECOVERY STRATEGY: ACROBOT VS. WOBBLE CHAIR

Hoda Koushyar, Christina Rossi

Virginia Tech, Blacksburg, VA

Abstract The human body can recover from an external perturbation using different balance recovery strategies. The strategy that the body chooses depends on factors such as the initial configuration of the body. Two configurations were modeled and studied in this paper. One configuration was representative of the body standing on a narrow beam (acrobat) and the other was the body sitting on an unstable chair (wobble chair). Both of these models were represented by topologically equivalent two segment inverted pendulums actuated only at the hip joint. Review of the literature hints towards the use of opposing strategies to recover from external perturbation however both models have yet to be examined systematically in a single study. Using a search method with variations in controller gains we revealed the presence of these opposing strategies in our model (acrobat vs. wobble chair).

Introduction

Single and multiple segment inverted pendulums have been used in biomechanics to evaluate and model balance recovery and postural control in humans when subjected to external or natural perturbations. Great insight can be gained from these models concerning the strategies used that govern the control of the body's center of mass (COM) over the base of support.

In the sagittal plane Nashner and McCollum showed that the body can be modeled as an under actuated double-segment inverted pendulum when a hip strategy is elicited to recover the location of the COM over the base of support [1]. This double inverted pendulum configuration is very similar to another device that is commonly referred to as an acrobot.

The term "hip strategy" refers to the use of torque actuation only at the hip joint to recover from a perturbation. The biomechanical model constrains the feet to be fixed to the ground and the knee to remain in a straight locked position. The use of this strategy was experimentally confirmed as the strategy a human uses to control balance in response to support translations during stance on a narrow beam [2].

It was examined that a forward or backward sway displacement at the base of support elicited a large active rotation of the hip joint that moved the trunk in the direction of the initial body displacement to a non-erect, however gravitational equilibrium, position (Figure 1). For future reference this will be referred to as strategy 1.
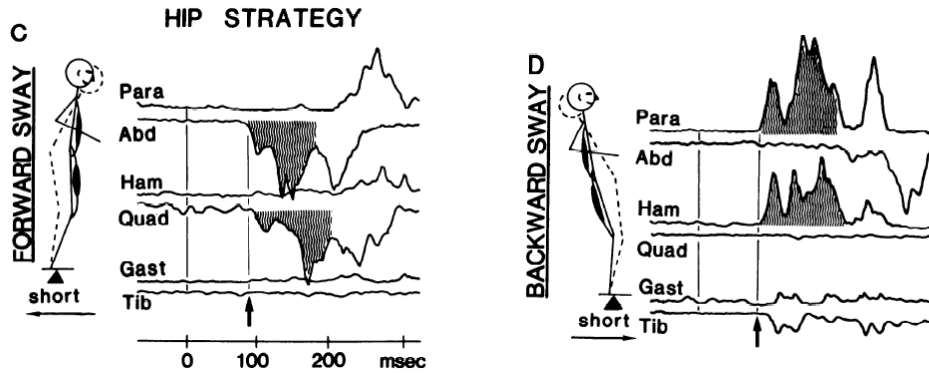
Figure 1: Displaying strategies used to recover from initial backward or forward sway perturbation while standing on narrow beams, Para,lumbar paraspinal muscles; Abd, rectus abdominis; Ham, hamstring; Qud, rectus femoris; Gast, medial gastrocnemius; Tib, tibialis anterior. The image shows little contribution from the Gast and Tib indicating the use of the hip strategy [2]

Another biomechanical model represented by a two segment inverted pendulum with motion restricted to the sagittal plane, evaluates seated stability using an apparatus termed a wobble chair [3]. The general description of the model is shown in Figure 2.


(a)
.
(b)
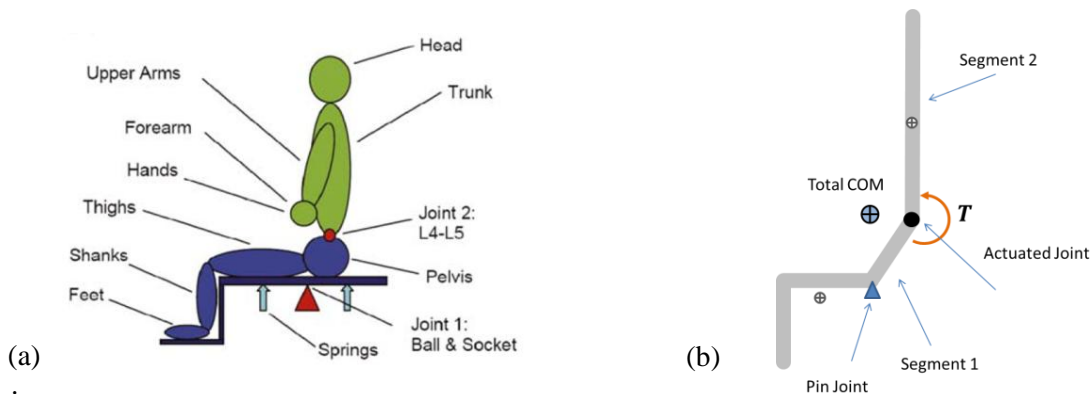
Figure 2: Wobble chair (a) [3], and associated two segment inverted pendulum model (b).

The upper segment of the inverted pendulum is representative of the head, arms and torso, while the lower segment is formed by the lower body in addition to the chair. It was shown by Tanaka et al. (2010) that this model is controllable with torque actuation being located only at the hip joint (the joint between the 4th and 5th lumbar vertebrae where most of the movement occurs), just like that of the acrobot model. For the wobble chair, the strategy to recover COM location was achieved by causing flexion of the trunk when the overall center of mass was posterior to the point of equilibrium and extension of the trunk when COM was anterior to the point of equilibrium [3]. This strategy, strategy 2, is opposite to the strategy used for the acrobot model.

Although both the acrobot and wobble chair are biomechanical models represented by double inverted pendulums they differ greatly in COM locations and review of the literature suggest they display opposite

strategies when recovering from applied perturbations. The difference between the strategies is shown in Figure3.
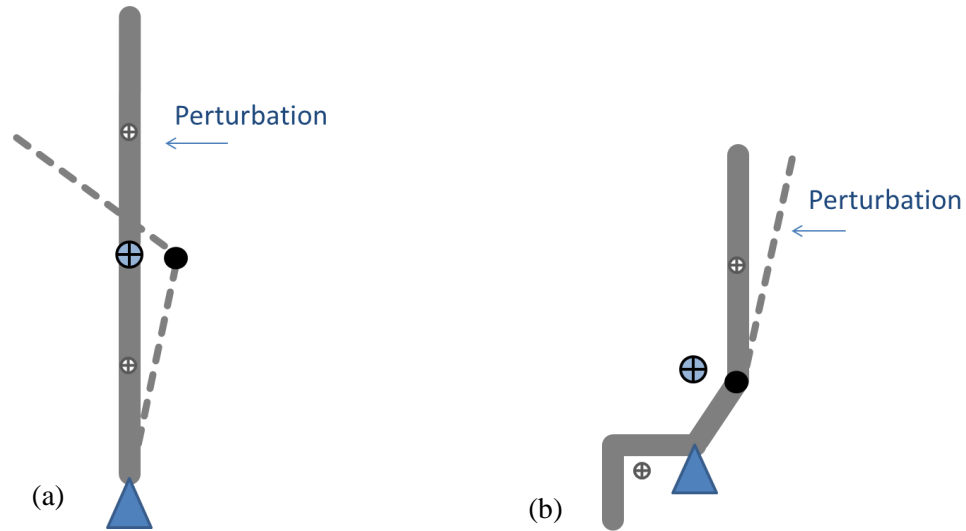
Figure 3. Differences in strategies between acrobot (a) and wobble chair (b) models. The standing acrobot model is displaying strategy 1 while the seated wobble chair model is displaying strategy 2. Dashed lines represent positions after recovery from the perturbation.

Although both the acrobot and wobble chair model have been examined in the literature, the difference in recovery strategy between the two has yet to be looked at. The purpose of this report is to attempt discovery, in a systematic manner, of the opposing strategies used between the wobble chair and the acrobot to recover balance after an external perturbation. An acrobot model, a wobble chair model, and several intermediate models were created and controlled using a proportional-integral-derivative controller (PID) and a comprehensive search of controller gains was performed to determine what strategies worked to stabilize and control the models.

Methods

Model Description

Since the acrobot and the wobble chair are from the same family of planar inverted double pendulums similar, however slightly modified, equations and methods can be used to represent both dynamic systems. As such, when explaining the construction of the models only the wobble chair will be discussed in detail, however it should be noted that the same equations were used in the construction of the acrobot. The schematic of the wobble chair is shown in Figure 4(a). The more detailed description of the first segment is shown in Figure 4(b).
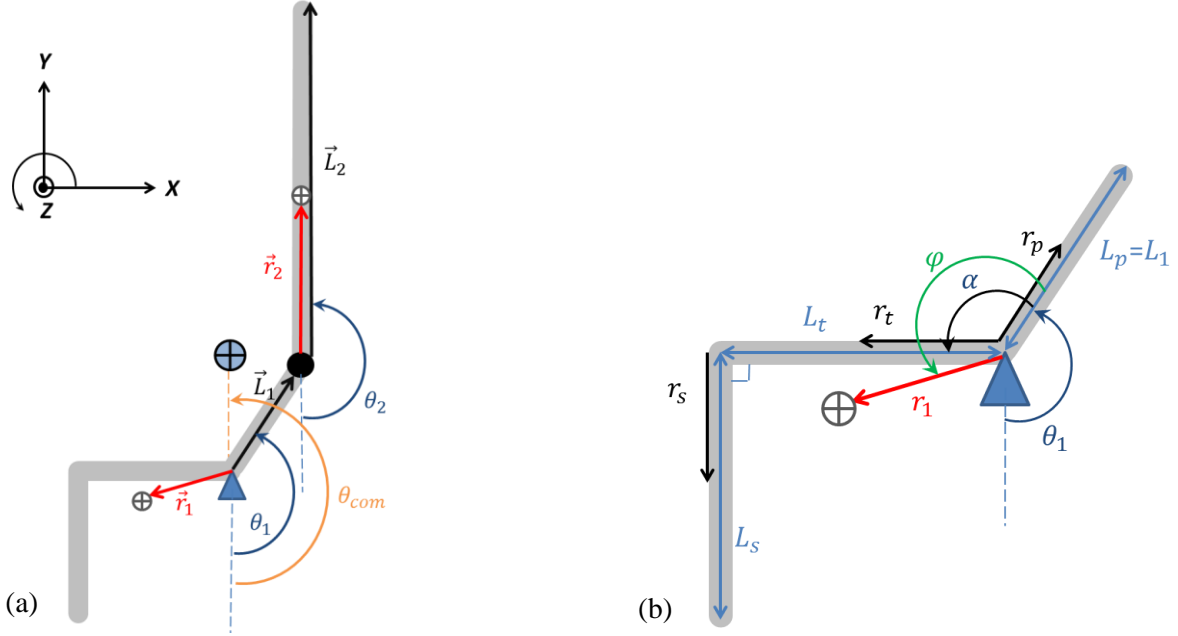
Figure 4: Wobble chair model description (a), geometric details of segment 1 (b)

The COM of each segment can be obtained by the following equations:

$$X_{COM_1} = (m_p * r_p * \sin\theta_1 + m_t * r_t * \sin(\theta_1 + \alpha) + m_s * (L_t * \sin(\theta_1 + \alpha) + r_s * \cos(\theta_1 + \alpha)))/(m_1) \qquad (1)$$

$$Y_{COM_1} = (-m_p * r_p * \cos\theta_1 - m_t * r_t * \cos(\theta_1 + \alpha) + m_s * (-L_t * \cos(\theta_1 + \alpha) + r_s * \sin(\theta_1 + \alpha)))/(m_1) \qquad (2)$$

$$X_{COM_2} = m_2(L_1 \sin\theta_1 + r_2 \sin\theta_2) \qquad (3)$$

$$Y_{COM_2} = -m_2(L_1 \cos\theta_1 + r_2 \cos\theta_2) \qquad (4)$$

Masses of the pelvis, thigh and shank are defined as $m_p, m_t,$ and $m_s,$ and the lengths are defined as $L_p, L_t,$ and L_s respectively. The COM of pelvis, thigh and shank are shown by $r_p, r_t,$ and r_s respectively. The sum of these masses is the mass of segment 1 (m_1). To be consistent with the definition of the segments r_p is called r_1 and L_p is called L_1 in the rest of the paper. The mass of segment 2 is defined as m_2 and the length of the segment is defined as L_1. The distance from the actuated joint to the COM of segment 2 is defined as r_2. The angles between the segment 1 and segment 2 and the vertical line, are $\theta_1,$ and θ_2 and α is the angle between the pelvis and the thigh.

Using the position of the first segment's COM, the global position of the following parameters can be found:

$$\varphi + \theta_1 = \tan^{-1}(X_{COM_1}/Y_{COM_1}) \qquad (5)$$

$$|r_1| = \sqrt{X_{COM_1}^2 + Y_{COM_1}^2} \qquad (6)$$

Where φ is the angle between the COM of segment 1, and segment 1 itself and r_1 is the distance from the pivot joint to the COM of segment 1.

Using the COM's of segment 1 and segment 2, the angle of the total COM can be determined as:

$$\theta_{COM} = \tan^{-1}(\frac{m_1*X_{COM_1}+m_2*X_{COM_2}}{m_1*Y_{COM_1}+m_2*Y_{COM_2}}) \qquad (7)$$

The value of θ_{COM} is the control parameter in the model and will be discussed in more detail in sections to follow.

The model of the acrobot is very similar to the wobble chair; however, φ and α are equal to zero, and segment 1 is a straight solid rod rather than a bent solid rod used in the wobble chair model (Figure 5).
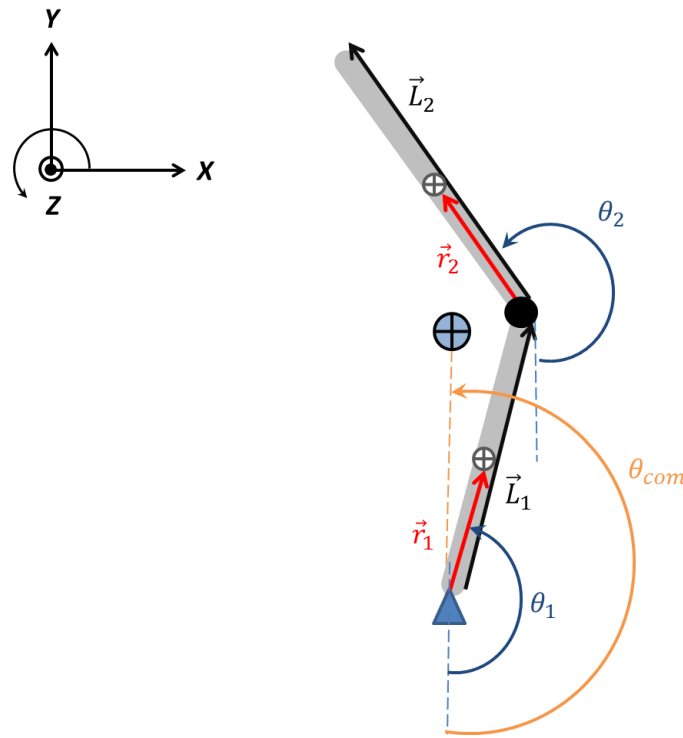
Figure 5: Acrobot model description and geometric details.

The parameter values used in this study for the acrobot and wobble chair models are shown in table 1.

Table 1. Acrobot and wobble chair model parameters

	m_p (kg)	m_t (kg)	m_s (kg)	m_1 (kg)	m_2 (kg)	r_1 (m)	r_2 (m)	L_1 (m)	L_2 (m)	I_1 (kg. m^2)	I_2 (kg. m^2)	α (deg)	φ (deg)
Acrobot	1	0	0	1	1	0.5	0.5	1	1	0.0833	0.0833	0	0
Whobble chair	0.2	0.4	0.4	1	1	0.195	0.5	0.2	1	0.0500	0.0833	150	176

Equations of motion (EQM)

The Lagrangian method was used to derive the EQM of the system.

$$\frac{d}{dt}\left(\frac{\partial L}{\partial \dot{q}_j}\right) - \left(\frac{\partial L}{\partial q_j}\right) = Q_j \qquad L = K - V \qquad \begin{aligned} q_1 &= \theta_1 \\ q_2 &= \theta_2 \end{aligned} \qquad (8)$$

Where K is the kinetic energy and V is the potential energy of the system and are calculated as:

$$K = \frac{1}{2}m_1|\dot{\vec{r_1}}|^2 + \frac{1}{2}m_2|\dot{\vec{r_2}}|^2 + \frac{1}{2}I_1\dot{\theta_1}^2 + \frac{1}{2}I_2\dot{\theta_2}^2 \qquad (9)$$

$$V = -m_1 g\,|\vec{r_1}|\cos(\theta_1 + \varphi) - m_2 g\,|\vec{L_1}|\cos\theta_1 - m_2 g\,|\vec{r_2}|\cos\theta_2 \qquad (10)$$

Using the kinetic and potential energy of the system, the equations of motion can be found as:

$$\boldsymbol{M\ddot{\theta} + C(\theta,\dot{\theta})\dot{\theta} + G(\theta) = Q} \qquad (11)$$

$$M = \begin{bmatrix} I_1 + m_1|\vec{r_1}|^2 + m_2|\vec{L_1}|^2 & m_2|\vec{L_1}||\vec{r_2}|\cos(\theta_1 - \theta_2) \\ m_2|\vec{L_1}||\vec{r_2}|\cos(\theta_1 - \theta_2) & I_2 + m_2|\vec{r_2}|^2 \end{bmatrix} \qquad (12)$$

$$C = \begin{bmatrix} 0 & m_2|\vec{L_1}||\vec{r_2}|\sin(\theta_1 - \theta_2)\,\dot{\theta_2} \\ -m_2|\vec{L_1}||\vec{r_2}|\sin(\theta_1 - \theta_2)\,\dot{\theta_1} & 0 \end{bmatrix} \qquad (13)$$

$$G = \begin{bmatrix} m_1 g|\vec{r_1}|\sin(\theta_1 + \varphi) + m_2 g|\vec{L_1}|\sin\theta_1 \\ m_2 g|\vec{r_2}|\sin\theta_2 \end{bmatrix} \qquad (14)$$

$$Q = \begin{bmatrix} -T + T_{sp} \\ T \end{bmatrix} \qquad (15)$$

The torque generated at the joint between the two segments is referred to as C_{pd}. The term T_{sp} refers to the torque created by a compression springs acting on the wobble chair. This torque is calculated as:

$$T_{sp} = k_s * d^2 * \sin(\theta_1) \qquad (16)$$

Where k_s is the spring constant and d is the acting distance. The spring constant is unique to the wobble chair model and represents the spring present in the actual wobble chair apparatus [4]. This parameter value was set as -10 N/m.

Controller

A PID controller was implemented to control the location of θ_{COM}. According to the Routh criterion for stability the *P* and *D* components of the controller are essential for stability of an inverted pendulum [5]. Jahansson et al. (1988) showed a biomechanical benefit of adding the third term *I*, which is proportional to the integral of the angular error signal [6].

In order for the system to achieve equilibrium the magnitude of θ_{COM} has to be zero, meaning the total COM of the connected system is balancing over the base of support. Consequently, the control error for the proportional, integral and derivative terms of the controller is the location of θ_{COM} the integral of

6

θ_{COM} and the derivative of θ_{COM} respectively (Figure 6). The proportional, derivative, and integral control gains, K_p, K_d and K_i were then used to obtain the torque required to bring the model to the stable position after the initial perturbation. The control equation and corresponding block diagram is as follows:

$$C_{pd} = K_d * \dot{\theta}_{COM} + \begin{cases} K_p * \theta_{COM} + K_d * \int_0^t \theta_{COM}\, dt & if \ |\theta_{COM}| < \theta_{critical} \\ T_{pmax} & Otherwise \end{cases} \qquad (17)$$
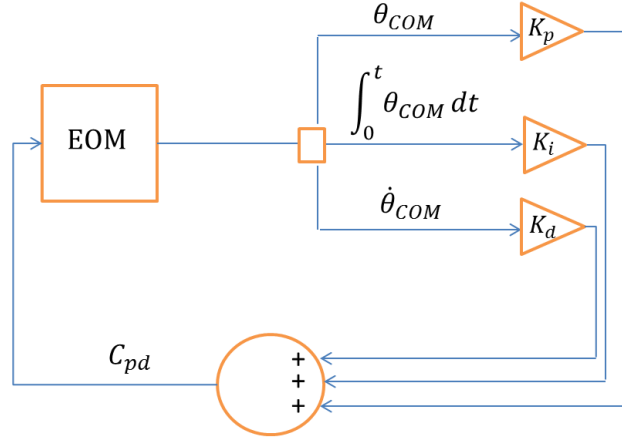
Figure 6: Block diagram showing closed loop feedback control

Physiologically, T_{pmax} characterizes the fact that muscle strength is limited. As a result, beyond certain values of θ_{COM}, the torque cannot be further increased. This value is calculated as $\theta_{critical} = \frac{T_{pmax}}{K_p}$ [7].

A comprehensive grid search was performed in all quadrants to evaluate stability results for all possible combinations of K_p and K_d. The grid search was created in Matlab and consisted of a for-loop that incremented K_p and K_d by 50 and 10 respectively for approximately 10,000 iterations in each of the four quadrants. Although the integral term has a biomechanical advantage, Maurer et al. (2005) showed that variations in the magnitude of K_i did not influence response results [8]. Suitably, the magnitude of K_i was kept at a constant value for the grid search.

Examining the equation for the control torque, it is easily seen that the sign of the controller gains has a direct relationship to the strategy used to recover from a perturbation. The prescribed perturbation for all models is a positive initial velocity equal to 0.1 rad/sec applied to the upper segment. This perturbation initially increases the magnitude of θ_{COM} hence making the proportional, integral and derivative of the control error (θ_{COM}) positive. If K_p, K_d and K_i are positive as well (corresponding to the 1st quadrant of grid search) the corrective control torque will be positive. This corresponds to strategy 1, in that the COM of the model is perturbed anteriorly and the hip joint moves the trunk in the direction of the initial body displacement. However, if K_p, K_d and K_i are all negative (making the control torque negative and corresponding to the 3rd quadrant of grid search) the opposing strategy, strategy 2, is used.

When examining the results for the grid search, it was established that, if the model showed stability in the first quadrant, strategy 1 was employed, if stability was seen in the third quadrant strategy 2 was

employed, and if stability was seen in quadrants 2 or 4 it was undetermined what strategy was used without closer assessment of the control torque at the corresponding stable location.

Stability

In order to determine the stability of the system at every combination of gains in the grid search, the Hilbert envelope method was used. This method was adapted from Tanaka et al. (2012) and determines stability by examining the expansion or contraction of oscillation magnitudes [7]. The complex analytical signal created by combining the Hilbert transform of a real function with its original signal is displayed below.

$$z(t) = a(t)e^{i\theta(t)} \qquad (18)$$

Where a(t) represents an envelope containing the oscillations of the original signal. Creating a linear fit for a(t) and observing the sign of the corresponding slope allows the stability of the system to be determined. A negative slope, as can be seen in Figure 7 shows a stable system indicating that the COM of the system is converging to zero. In opposition, a positive slope indicates an unstable system.
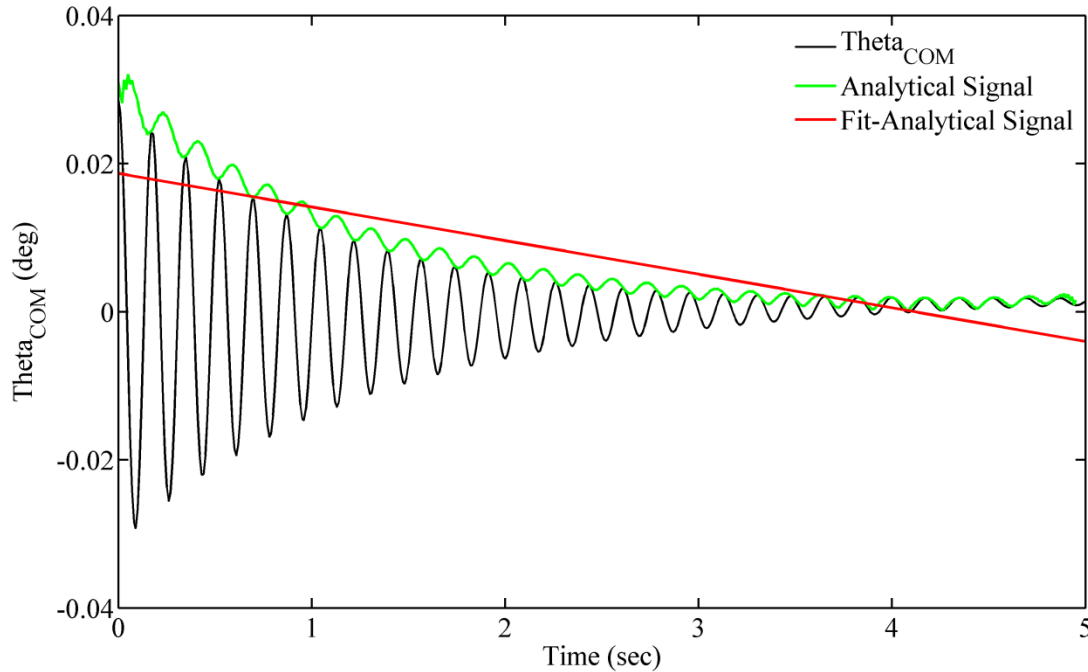

Figure 7: Hilbert envelope. Green represents the analytical signal and red represents the fit to this analytical signal. The slope of the linear fit is negative indicating a stable system.

Results

The results for the grid search show that the acrobot model (red) was stable in the first quadrant only and the wobble chair model (green) was stable in the third quadrant only (Figure 8). This indicates that the acrobot shows stability when recovering from a perturbation using strategy 1, and the wobble chair when using strategy 2. Neither model show areas of overlap where both strategies can be used to produce stable results.
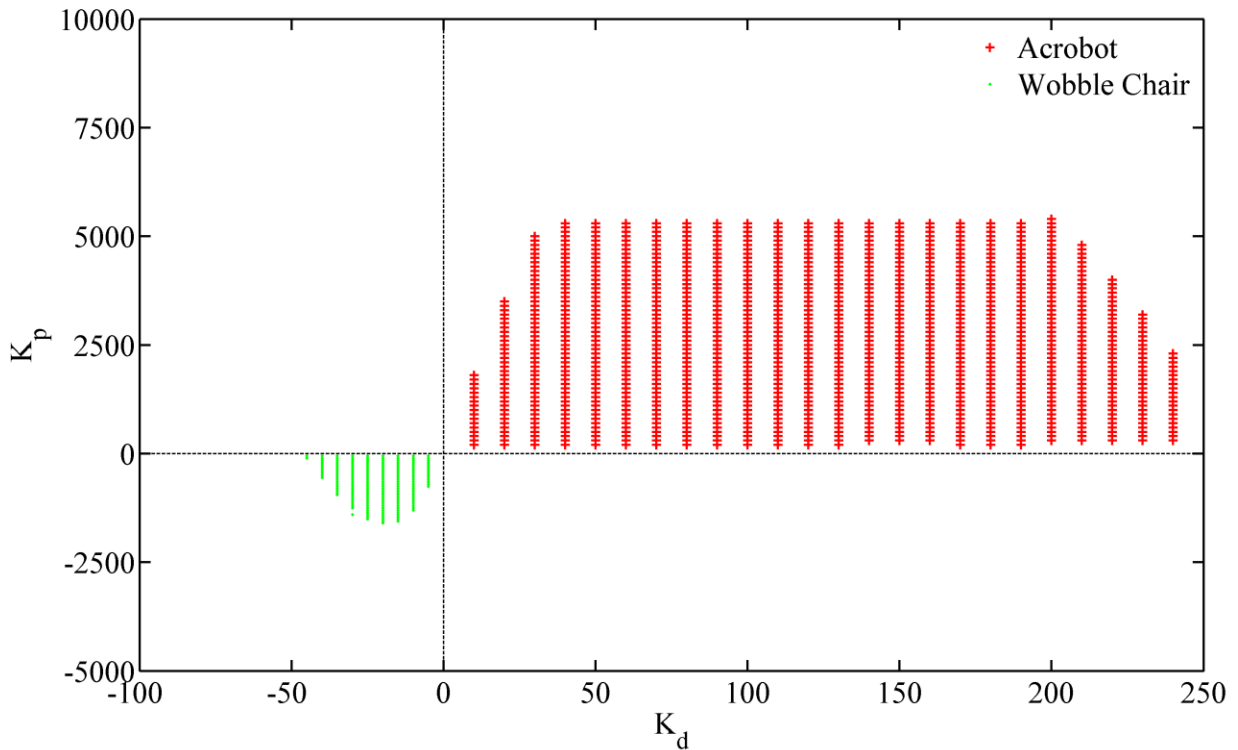

Figure 8: Results from the grid search for the acrobot and wobble chair models. Red represents acrobot results and green represents wobble chair results.

An additional indication that the two models are using opposite strategies can be seen by comparing the control torque with the location of θ_{COM} during the simulation. For the acrobot model (Figure 9) it is easily seen that the control torque is in phase with θ_{COM}. This specifies that when θ_{COM} is perturbed from the initial position the control torque responds by applying a torque in the same direction, representative of strategy 1. On the contrary, for the wobble chair model (Figure 10) the control torque is out of phase with the location of θ_{COM} which is representative of strategy 2.
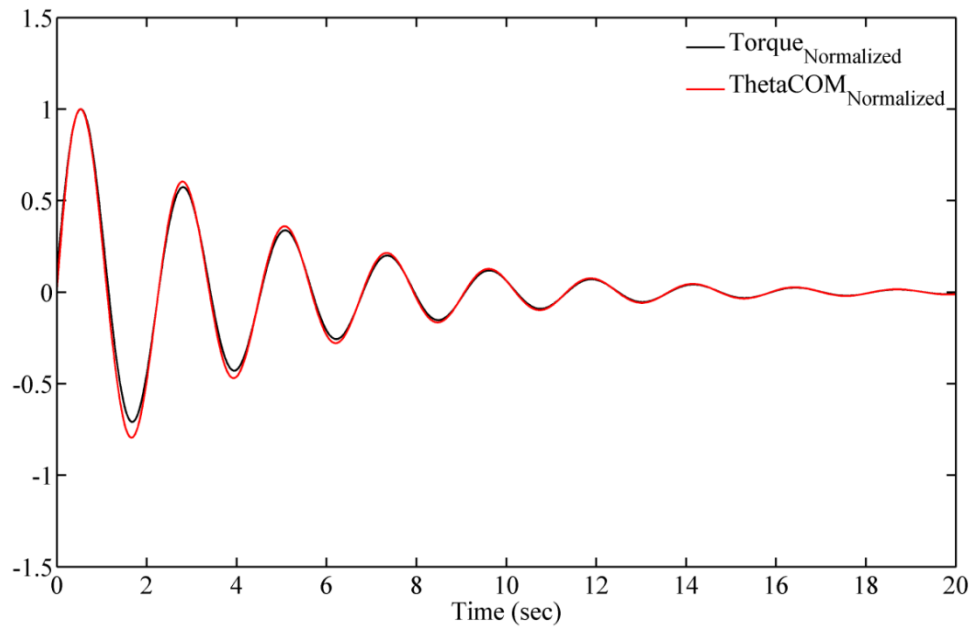
Figure 9: Acrobot model showing control torque in phase with θ_{COM} indicating use of strategy 1. Y axis shows the normalized values of torque and θ_{COM} to their peaks over time. The gains for this simulation were; Kp= 150 Ki=400 Kd=150
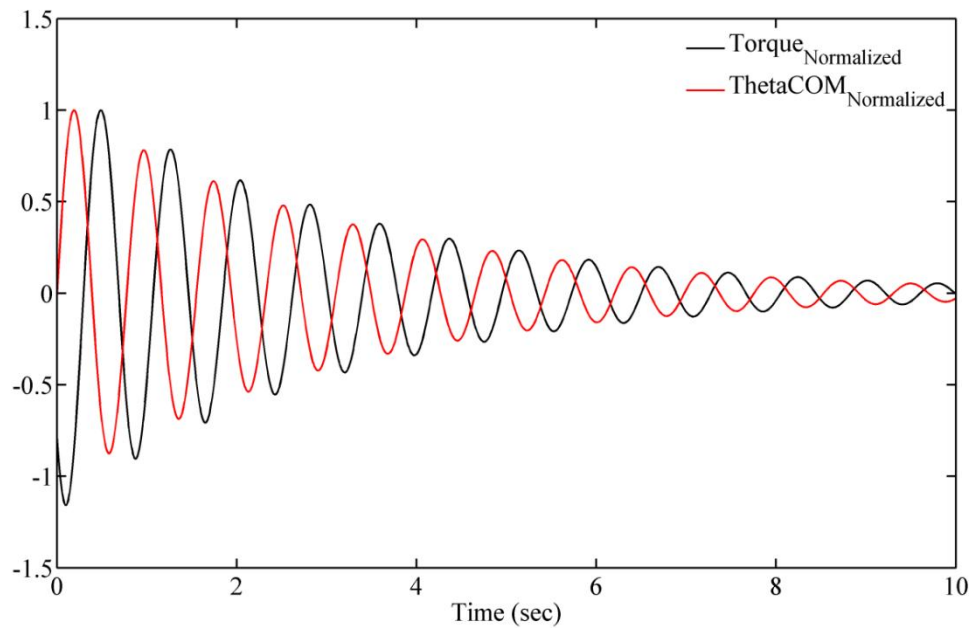

Figure 10: Wobble chair model showing control torque out of phase with θ_{COM} indicating use of strategy 2. Y axis shows the normalized values of torque and θ_{COM} to their peaks over time. The gains for this simulation were; Kp= -50 Ki=-400 Kd=-10

Discussion

Although the two recovery strategies are clearly different between the models, why the models choose the strategies they do is still fairly unclear. There are several proposed methods for examining this phenomenon and we have completed a preliminary investigation on a few that are worth mentioning.

One of the key differences between the acrobot and the wobble chair is the location of the COM of segment 1 (Figure 11). As can be seen in Figure 11 two discrete things happen to the COM of segment 1 as you transform from acrobot to wobble chair; the COM moves away from the segment horizontally, and the COM moves down vertically towards, and eventually under, the pivot point. If this is the main determinant of what strategy is being used, slowly manipulating the location of this COM and determining stability at intermediate locations may give insight into when and why the strategies change.
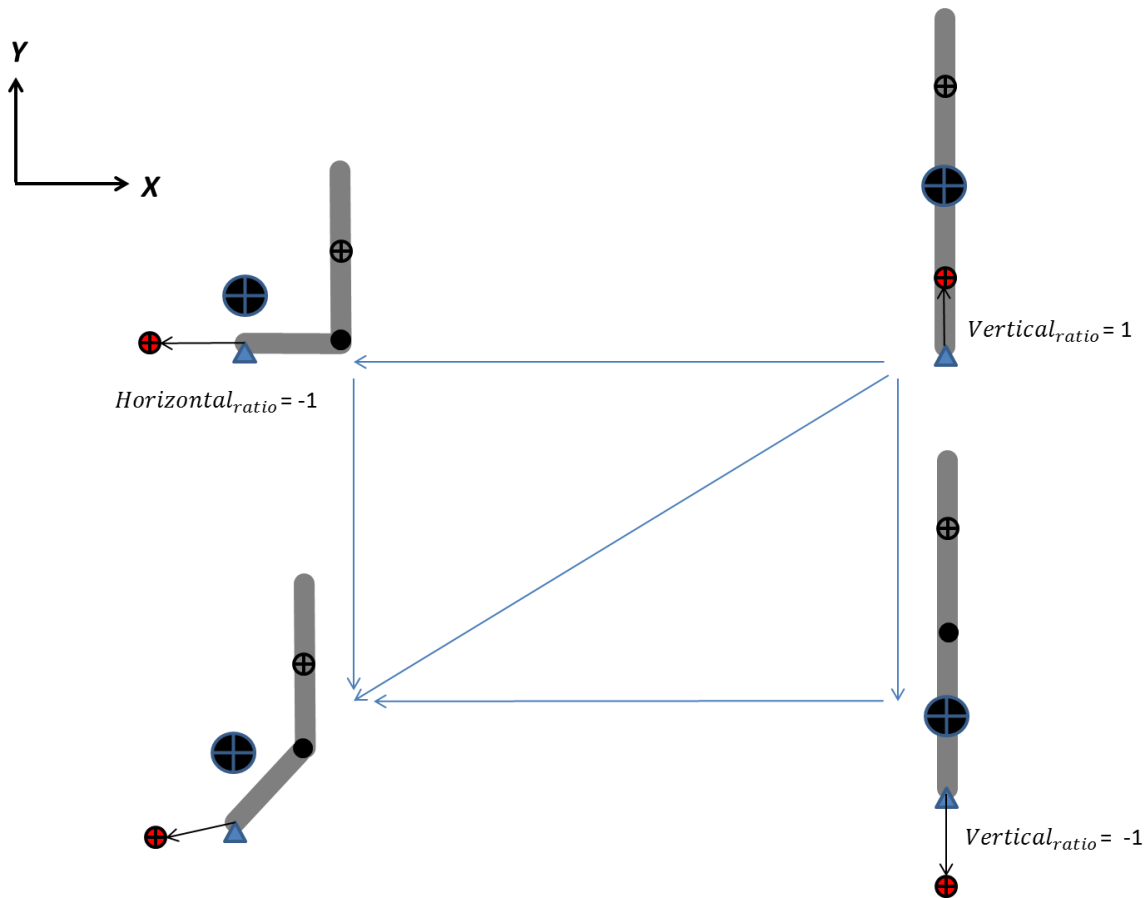
Figure 11: Display of the transition the COM of segment 1 goes through when transforming from acrobot to wobble chair.

As an initial approach, the model was slowly transformed from the acrobot to the wobble chair along the diagonal of Figure 11 using a continuous transformation variable x (Figure 12).
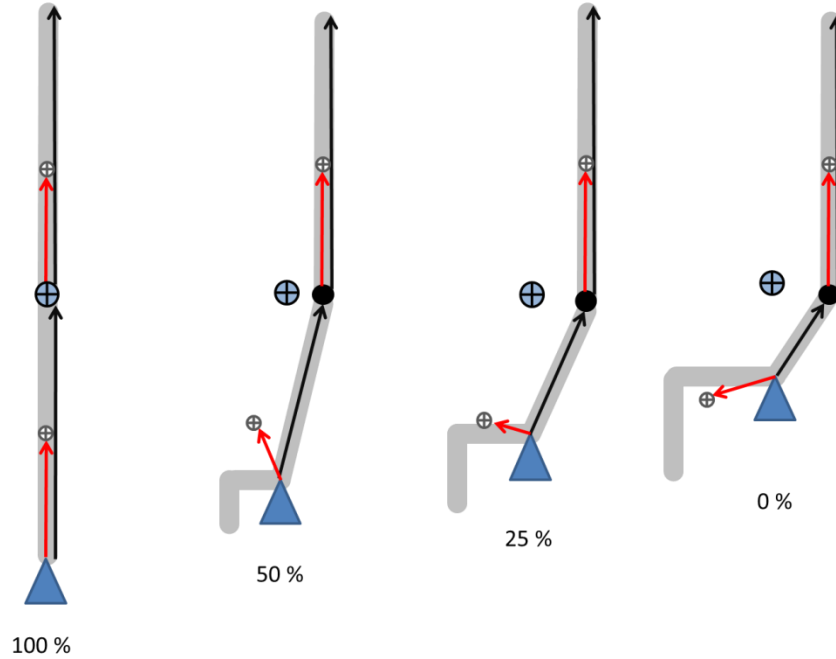
Figure 12: Transformation from acrobot to wobble chair. This figure shows intermediate models of 50% and 25% acrobot.

The transformation equation for the length and mass of segment 1 is shown below. The length and mass of segment 2 was constant throughout the transformation.

$$L_1 = L_{1A}(x) + L_{1S}(1 - x) \qquad (19)$$

$$m_1 = m_{1A}(x) + m_{1S}(1 - x) \qquad (20)$$

L_{1A}, L_{1S}, m_{1A} and m_{1S} are the lengths and masses of segment 1 in the original acrobot and wobble chair models respectively. It is easily seen from this equation that if the transformation variable x is equal to 1 this corresponds to a model that is 100% acrobot. The same equation was applied to the spring constant k_s, so that when the model was 100% acrobot k_s was equal to 0.

To take into account the addition of the shank and thigh as you transform to the seated position, L_1 and m_1 were calculated with the equations above and assigned to be equal to the length and mass of the pelvis segment only. The length and mass of the shank and thigh segments were then determined such that

$$L_t = L_s$$

$$m_t = m_s$$

$$1 = L_p + L_s + L_t$$

$$1 = m_p + m_s + m_t$$

This was to insure that the total mass of the model remained constant throughout the transformation so not to confound results.

When running a full grid search for the transformed models there were zero points of stability for models representing 75%, 50% and 25% acrobot. Stability regions were found in the third quadrant for 15% and 10% acrobot. These regions of stability are shown in Figure 13 below.
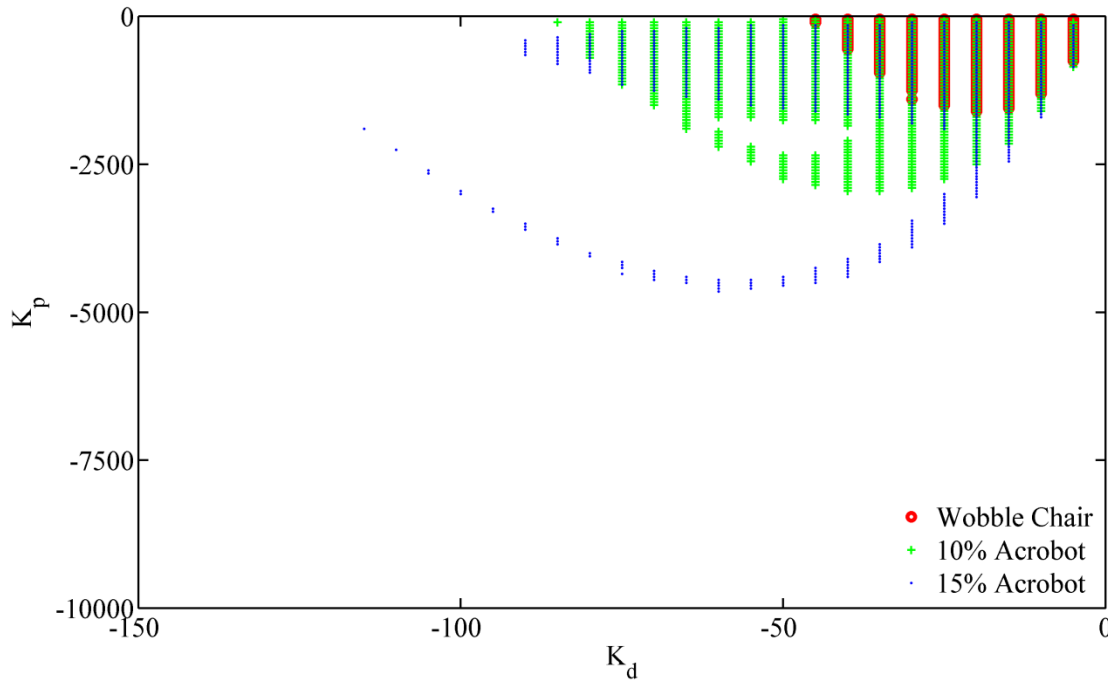
Figure 13: Grid search results for 10% (green) and 15% (blue) acrobot. Results for original wobble chair are also displayed (red)

Transformations above 15% acrobot put the COM of segment 1 above the pivot point. Speculation suggests that the location of segment 1's COM below the pivot point may be a determining factor in the strategy the model chooses to use. It is unclear however why there are no stable regions in any quadrant for transformed models above 15%. If the location of the COM of segment 1 with respect to the pivot point is determinant of strategy, one would predict stable regions in the first quadrant for the transformations above 15%. Future work could be done to determine why this occurs.

Rather than moving diagonally down toward the wobble chair, another approach to determine if the location of the COM of segment 1 is depicting strategy is to move the COM along the x and y axis of Figure 11 independently. This may determine if the recovery strategy is dependent on moving the COM horizontally or dependent on moving it vertically with respect to the pivot point. Future work will be done to create these transformed models and determine stability regions.

Another evident difference between the two models is the use of stabilizing springs in the wobble chair. One may reason that this is a factor for the change in strategy such that the springs are influencing the direction the control torque is applied. Removing the springs from the wobble chair model however produces no stable results for the grid search, possibly due to the offset locations of the COM of the upper and lower segment. As a result, in order to test this hypothesis springs had to be added to the acrobot model so that the two models could be equally compared. Results for the acrobat model with an added

spring were identical to those for the acrobat without the spring. This suggests that the presence of the spring in the wobble chair model is not a depiction of the recovery strategy used.

Conclusion

It was hypothesized from the results of previous research that the two double inverted pendulum models recover in opposite manners. The results from the comprehensive grid search performed in this study showed that not only do the models recover using opposing strategies; the models are incapable of recovery using the same strategy. It is still unclear as to why this is, however future work will be done to transform the model in different ways in order to pinpoint the exact cause of this phenomenon.

References

1. Nashner L, McCollum G. The organization of human postural movements: a formal basis and experimental synthesis. Behav Brain Sci 1985;8:135-72
2. Horak F, Nashner L. Central programming of postural movements: adaptation to altered support-surface configurations. J Neurophysiol 1986;55(6):1369-81
3. Tanaka, M, Ross S, Nussbaum M. Mathematical modeling and simulation of seated stability. J Biomechanics 2010;43:906-12
4. Slota, G., K. Granata, and M. Madigan. Effects of Seated Whole-body Vibration on Postural Control of the Trunk during Unstable Seated Balance. Clinical Biomechanics 2008;23:381-86
5. Hahn, W. Stability of Motion;. Berlin: Springer-Verlag, 1967. Print
6. Johansson R, Magnusson M, Akesson M. Identification of human postural dynamics. Transaction on Biomedical Engineering 1988;35(10):858-69
7. Tanaka M, Ross S. Using topological equivalence to discover stable control parameters in biodynamic systems. Comp Methods in Biomech and Biomed Eng. 2012;15(8):875-84
8. Maurer C, Peterka R. A new interpretation of spontaneous sway measures based on a simple model of human postural control. J Neurophysiol 2005;93:189-200